

Estimating trends in the global mean temperature record

Andrew Poppick*

Department of Mathematics and Statistics, Carleton College,
Elisabeth J. Moyer

Department of the Geophysical Sciences, University of Chicago
and

Michael L. Stein

Department of Statistics, University of Chicago

December 9, 2021

Abstract

Physical models suggest that the Earth’s mean temperature warms in response to changing CO₂ concentrations (and hence increased radiative forcing); given physical uncertainties in this relationship, the historical temperature record is a source of empirical information about global warming. A persistent thread in many analyses of the historical temperature record, however, is the reliance on methods that appear to deemphasize both physical and statistical assumptions. Examples include regression models that treat time rather than radiative forcing as the relevant covariate, and time series methods that account for natural variability in nonparametric rather than parametric ways. We show here that methods that deemphasize assumptions can limit the scope of analysis and can lead to misleading inferences, particularly in the setting considered where the data record is relatively short and the scale of temporal correlation is relatively long. A proposed model that is simple but physically informed provides a more reliable estimate of trends and allows a broader array of questions to be addressed. In accounting for uncertainty, we also illustrate how parametric statistical models that are attuned to the important characteristics of natural variability can be more reliable than ostensibly more flexible approaches.

Keywords: Climate change; climate sensitivity; time series; parametric modeling; bootstrap.

*The authors thank Jonah Bloch-Johnson, Malte Jansen, Cristian Proistosescu, and Kate Marvel for helpful conversations and comments related to parts of this work. This work was supported in part by STATMOS, the Research Network for Statistical Methods for Atmospheric and Oceanic Sciences (NSF-DMS awards 1106862, 1106974 and 1107046), and RDCEP, the University of Chicago Center for Robust Decision Making in Climate and Energy Policy (NSF Grant SES-0951576). We thank NASA GISS, NOAA, the Hadley Centre, the IPCC, and IIASA for the use of their publicly available data. We acknowledge the University of Chicago Research Computing Center, whose resources were used in the completion of this work.

1 Introduction

The physical basis of climate change is understood through a combination of physical theory, numerical simulations, and analyses of historical data. A fundamental concept to explain global warming is that of *radiative forcing*, which is the change in net radiation (downwelling minus upwelling, typically expressed in units of W/m^2 , at the top of atmosphere) resulting from an imposed perturbation of a climate in equilibrium, such as a change in the atmospheric concentration of a greenhouse gas. An increase in atmospheric CO_2 , for example, reduces upwelling radiation and produces a net influx of heat; the Earth's surface then warms until radiative equilibrium is restored. The most important source of forcing in the present climate is anthropogenic emissions of CO_2 , but other anthropogenic or natural forcing agents also contribute to climate change. (Anthropogenic agents include more minor greenhouse gases and aerosols; natural agents include aerosols from volcanic eruptions and periodic variations in solar insolation.) The Earth's response to forcing is complex and not fully understood, as there are physical uncertainties in important feedbacks such as cloud responses. A comprehensive source of information about climate change can be found in the assessment reports of the Intergovernmental Panel on Climate Change (IPCC) (the most recent being IPCC (2013)).

Given these physical uncertainties, the observed global mean temperature record since the late nineteenth century is a source of empirical information about the Earth's systematic response to forcing. (Figure 1 shows one estimate of annually averaged global mean surface temperatures from the past 136 years along with estimates of radiative forcings from various constituents during that period, with the data sources described in Section 2.) Analysis of the observed temperature record is complicated by the short available record of direct measurements, by uncertainties in the historical radiative forcings themselves, and by the natural temperature variability that exists even in the absence of forcing. Statistical methods are required to quantify the information in the historical record about the response to forcing: given the data, what do we know about how global temperatures have warmed in response to forcing, how much warming can we expect in plausible future forcing scenarios, and how do we expect uncertainties to change as we continue to observe the Earth's temperatures?

One common approach to using the observed temperature record to understand aspects of climate change is to assume a physical model of the system. Such a model can range from a simple energy balance model to a very complicated atmosphere-ocean general circulation model (GCM). Examples of analyses of observed temperatures using simple or moderately complex physical models to estimate expected changes due to forcing include Gregory et al. (2002), Forest et al. (2006), Gregory and Forster (2008), Padilla et al. (2011), Aldrin et al. (2012), Otto et al. (2013), Masters (2014), Lewis and Curry (2015), and many others; see also IPCC (2013) Chapter 10 and references therein for methods using GCMs.

Other approaches are more empirical and appear to deemphasize assumptions about the underlying physics generating the observed temperatures. These ostensibly objective analyses can involve both parts of the statistical modeling endeavor, i.e., characterizing both the systematic response and the natural variability. First, in modeling the systematic response of temperatures over time, it is somewhat common practice to use regression models that treat time rather than radiative forcing as the covariate. Studies that incorporate this practice into analyses testing for either significant warming or changes in warming trends include Bloomfield (1992), Smith and Chen (1996), Foster and Rahmstorf (2011),

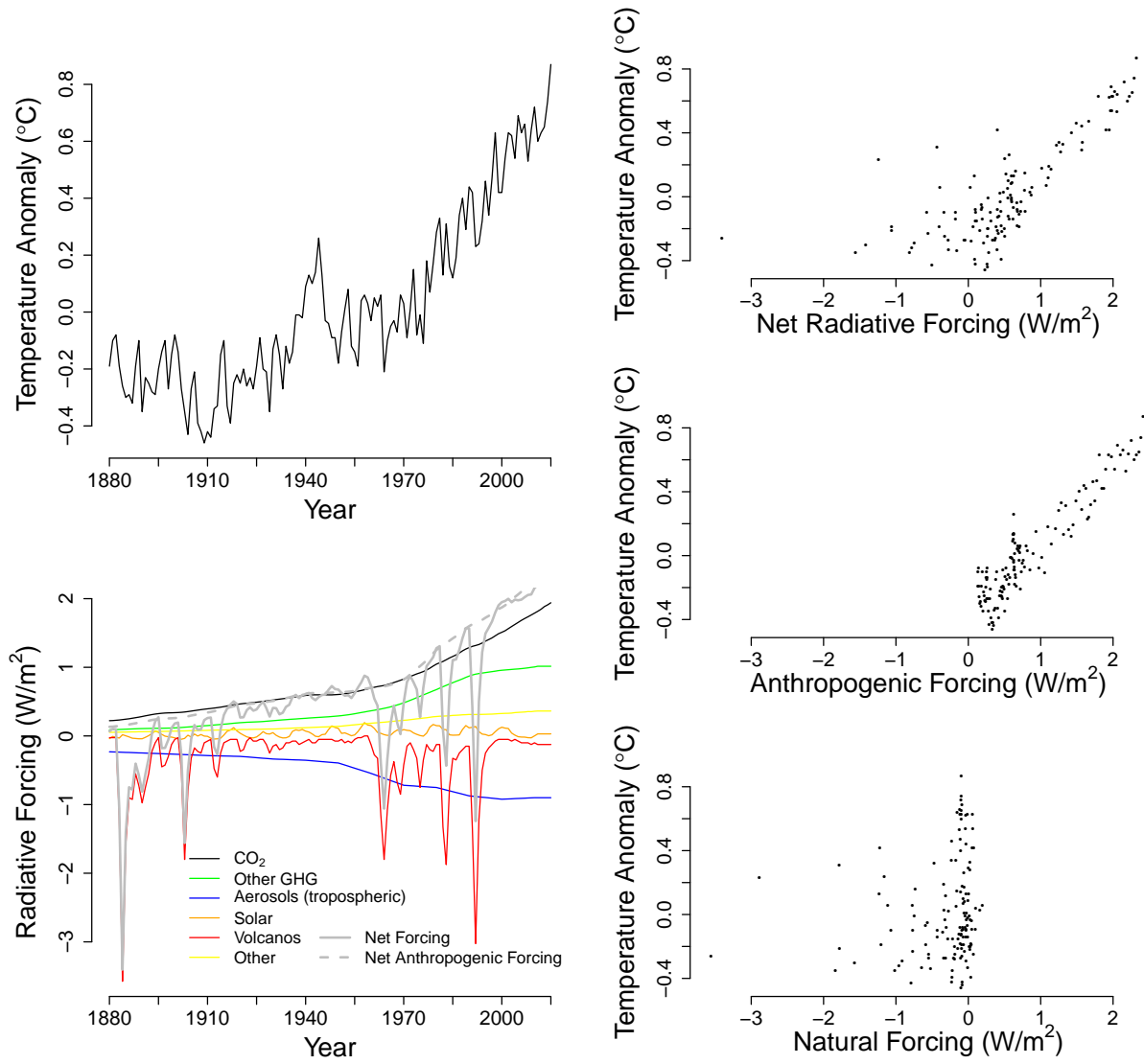


Figure 1: Top left, estimates of annually averaged global mean surface temperature anomalies (relative to a base period of 1951-1980) from the years 1880 to 2015. Bottom left, estimates of (top-of-atmosphere) effective radiative forcings from different constituents over this time period (the “other” category includes O₃, H₂O, black carbon, contrails, and land use changes). Right, temperature anomalies vs. net radiative forcings (top), vs. anthropogenic forcing (middle), and vs. natural forcing (bottom). Data sources are described in Section 2. Despite the plots of temperature vs. radiative forcing, temperatures will depend on the full past trajectory of radiative forcings in a potentially complex way, as we discuss in Section 3.

Cahill et al. (2015), Rajaratnam et al. (2015), and Løvsletten and Rypdal (2016), and many others. (See also IPCC (2013), especially Chapter 2 Box 2.2, and references therein.) Second, in coping with natural variability for the purpose of uncertainty quantification, some authors prefer nonparametric (resampling or subsampling) methods for time series over parametric approaches (such as assuming an autoregressive moving average (ARMA) model with a small number of parameters) (e.g., Gluhovsky (2011) and Rajaratnam et al. (2015)).

We argue that methods that deemphasize assumptions can be problematic in this setting. While regressions in time are simple to apply and do not appear to make explicit assumptions about how temperatures should respond to forcing, these models both limit what can be learned from the data and can lead to misleading inferences. They are sensitive to arbitrary choices (such as the start and end date of the data analyzed), cannot be expected to apply over even modestly long timeframes, and cannot in general reliably separate trends of interest from natural variability. Furthermore, in accounting for natural variability, nonparametric methods for time series often require long data records to work well, and can be seriously uncalibrated in more data-limited settings such as the one we are discussing.

In the following, we show that (a) targeted parametric mean models that incorporate even limited physical information can provide better fitting, more interpretable, and more illuminating descriptions of the systematic response of interest compared to approaches that deemphasize assumptions, and (b) parametric models for residual variation can provide for safer and more accurate uncertainty quantifications in this setting than do approaches that deemphasize assumptions, especially if the parametric modeling is done with particular attention towards the representation of low-frequency natural variability. We believe that the analysis that we present is informative, even if not maximally so, and we attempt to highlight both complications with our analysis as well as important sources of information about global warming that are ignored in our approach. Our goals are to indicate directions in which statisticians can incorporate explicit modeling to positive effect and to highlight what we view are some of the important sources of uncertainty and information in this problem.

This article is organized as follows. In Section 2, we introduce the data sources used in our analysis. In Section 3, we provide some background on modeling the historical global mean temperature record and contrast a proposed, minimally physically informed model with a more empirical approach. In Section 4, we highlight insights that can be gained from the more informed approach, with an emphasis on probing different aspects of uncertainty in trends. In Section 5, through synthetic simulations, we compare the performance of various parametric and nonparametric methods of uncertainty quantification in the presence of temporal correlation in settings similar to that of the historical temperature record. In Section 6, we give some concluding remarks. Additional material may be found in the appendix.

2 Background and data

Our analysis requires estimates of historical global mean temperatures and radiative forcings. To the extent that we are interested in how temperatures may evolve in the future (and how uncertainty in the response to radiative forcing evolves as more data is observed),

we also need radiative forcings associated with a plausible future scenario.

Temperature. We use the Land-Ocean Temperature Index from the NASA Godard Institute for Space Studies (GISS) (Hansen et al., 2010) in our primary analysis¹. The index combines land and sea surface temperature measurements to estimate annual average global mean surface temperature anomalies (relative to a base period from 1951-1980), extending from the year 1880 to the present (comprising 136 years in total). Any dataset of global mean temperature anomalies represents an estimate of that quantity and is subject to some uncertainty. Sources of uncertainty include the spatial coverage of the network of measurements, interpolation schemes used to estimate temperatures at unobserved locations, methods used to incorporate different sources of data (e.g., land- vs. satellite- vs. surface buoy- vs. ship-based data), and instrumental errors. Sources of uncertainty in the GISS dataset are discussed in Hansen et al. (2010). NASA GISS has made some attempt to provide pointwise uncertainty estimates for their data (e.g., Figure 9(a) of Hansen et al. (2010)), but it is important to realize that errors will be correlated in time. That said, uncertainties in the temperature record are relatively small compared to the changes in temperatures observed over the 20th century.

Different global observational datasets exist. At least one other popular source, the Hadley Centre’s HadCRUT4 product, is released as an ensemble of estimates in an attempt to explicitly account for uncertainty (Morice et al., 2012)². (A brief comparison of these two sources, as well as one from the National Oceanographic and Atmospheric Administration (NOAA), can be found in IPCC (2013), Section 2.4.3.) We repeat a small portion of our analysis using the HadCRUT4 global annual temperature ensemble (Section 4.5).

Radiative forcing. The primary driver of climate change during the observed period is changing atmospheric CO₂ concentrations; radiative forcing scales approximately with the logarithm of the fractional change in CO₂ concentrations from the preindustrial level (e.g. Arrhenius (1896) and many others). However, as discussed above, other agents also have radiative forcing effects (e.g., aerosols from human sources or volcanoes, other greenhouse gasses, etc.). These effects are typically described in terms of their *effective radiative forcing*, which is the radiative imbalance after rapid atmospheric adjustments and is intended to partially compensate for differing efficacies of forcing agents. In practice, effective forcings are often treated as though they may be combined additively. For effective radiative forcings from 1750-2011, we use the estimates in IPCC (2013) Table AII.1.2 (Figure 1 only shows the forcings after 1880, but the full available record is used in our analysis); from 2011-2015, we use the global CO₂ concentrations from NOAA³, and assume radiative forcing from other sources is constant during this period.

While the concentrations of well-mixed greenhouse gasses like CO₂ are relatively easy to measure, other forcing agents, such as tropospheric aerosols, are more difficult because they are spatially heterogenous and short-lived. Uncertainties in tropospheric aerosols are important because aerosol effects can be negatively confounded with greenhouse gas effects (see Figure 1, bottom left). Generally, uncertainties vary by constituent, as does the extent to which the estimates are derived from model output versus observations; see IPCC (2013) Chapter 8. The focus of this paper is on the information content of the observed temperatures assuming known forcings, but we make a limited attempt to discuss the effect

¹This dataset is updated periodically; the data we analyze was accessed on the date 2016-02-03. The current version is available at <http://data.giss.nasa.gov/gistemp/>

²Available here: <http://www.metoffice.gov.uk/hadobs/hadcrut4/data/current/download.html>

³See: ftp://aftp.cmdl.noaa.gov/products/trends/co2/co2_annmean_gl.txt

of uncertainty in the forcings (Section 4.5).

For a plausible future radiative forcing scenario, we use the Representative Concentration Pathway scenario 8.5 (RCP8.5) (Riahi et al., 2011; Meinshausen et al., 2011)⁴, where the change in radiative forcing from the preindustrial level is 8.5 W/m² by the year 2100 and in the extended scenario levels off at the year 2250. In our simulations, we slightly rescale the radiative forcings from the RCP8.5 scenario in the 21st century to match what we take to be the historical value in 2015, and we assume that natural forcings remain constant after 2015.

3 Modeling trends in the observed global mean temperature record

Evaluating the systematic response of global mean surface temperatures to forcing is complicated by the long timescales for warming of the Earth system. Because the Earth’s climate takes time to equilibrate, the near-term (transient or centennial-scale⁵) climate response will be less than the long-term (equilibrium or millennial-scale) response. The evaluation is also complicated by the fact that historical radiative forcings are not constant but rather evolve in time (e.g., atmospheric CO₂ increases). The physical lags in response imply that the Earth’s global mean temperature at any given time depends on the past trajectory of radiative forcings (because the climate does not instantly equilibrate to the present forcing).

A common framework is to decompose observed temperatures into two components: a systematic component changing in response to past forcings and a residual component representing sources of natural variability. That is, for global mean temperatures $T(t)$ at time t ,

$$T(t)|\{F(t'); t' \leq t\} = f(F(t'); t' \leq t) + \epsilon(t), \quad (1)$$

where f is an unknown functional of $\{F(t'); t' \leq t\}$, the collection of past radiative forcings associated with each forcing agent, and where $\epsilon(t)$ is a residual process that is mean zero and correlated in time. The problem, then, is how to estimate the systematic response f .

3.1 Regression models in time

Estimating a model like (1) is intractable without additional assumptions. As discussed above, one approach is to resort to physical models. But if instead a more empirical analysis of the observed data is desired, it is common practice to consider a surrogate regression on time itself, as stated in Section 1. The implicit assumption here is that, when viewed as a function of time, the systematic response to historical radiative forcings is approximately linear in time, at least over the considered timeframe:

$$f(F(t'); t' \leq t) \approx \alpha + \beta t, \quad t \in [t_0, t_1] \quad (2)$$

where α and β are unknown parameters and the trend is considered over the interval $[t_0, t_1]$. The linear time trend approach arguably involves assumptions about the forcing history

⁴See: <http://tntcat.iiasa.ac.at/RcpDb>

⁵Since the term *transient climate response* has a specific definition in the literature (see Appendix A1 for a discussion), we use the term *centennial-scale response* to describe the systematic response of temperatures to forcings on the mixing timescale of the mixed layer of the ocean but not of the deep ocean.

in addition to the systematic response f , since it will be a closer approximation when the forcing itself evolves linearly in time.

The linear time trend model is widely used, and the general sense is that such a model offers a way of testing for significant changes in mean temperature without having to make physical assumptions and without having to believe that the true response is linear in time (e.g. Bloomfield (1992) and Løvsletten and Rypdal (2016)). The IPCC, accounting for the apparent appeal of the linear time trend model, writes that it “is relatively simple, transparent and easily comprehended, and is frequently used in the published research assessed here,” (IPCC (2013) Chapter 2, Box 2.2), but suggests that linearity in time can at best be viewed as an approximation expected to hold over a relatively short period of time. Neither the observed temperature record nor the forcing history appear to evolve linearly over the full range of the data record (Figure 1, left).

While the time trend model may be routine to apply, appear objective, and provide a good fit to the data, its use can be precarious. A proper accounting of uncertainty in mean temperature changes relies on distinguishing natural variability from systematic responses. The time trend model is problematic in this respect. If the chosen time interval is short, it can be difficult to distinguish between trends and sources of natural variability that are correlated over longer timescales than the chosen interval (implicit in, e.g., Easterling and Wehner (2009) and Santer et al. (2011)). If the chosen interval is long and the systematic trend is actually nonlinear in time, then assuming a linear model in time will shift part of the systematic response to the residual process and can therefore give the impression of excessive natural variability over long timescales (and hence excessive uncertainty in trends).

Because the time trend model cannot be applied over long time intervals for arbitrary forcing scenarios, it also does not have a property that may be considered important for making inferences: that we can learn more about the systematic trend of interest by collecting more observations. There will be only a finite amount of information about the systematic response within the interval $[t_0, t_1]$ (this because sources of natural variability will be positively correlated in time). While this on its own does not invalidate the use of such a model over some narrow time frame, it does mean that what can be learned from the linear time trend model is necessarily limited. More broadly, since the linear time trend model does not map to a physical understanding of the relationship between radiative forcing and global mean temperatures, either during the time interval $[t_0, t_1]$ or extending beyond it, the questions that can be asked with this model are narrow.

Some argue that many of these problems may be overcome by using a model that is nonlinear in time, such as a spline or other nonparametric regression method. (The IPCC, for example, appears to view nonparametric extensions as more generically appropriate than the linear model.) Nonparametric regressions in time will appear to provide an even better fit to the data than the linear trend model, but many of the above arguments carry over to this setting. Such models have limited interpretational value and cannot generically be expected to distinguish between the systematic trends of interest and other natural sources of long-timescale variation in the data. Collectively, these arguments suggest that it is advisable to seek better motivated models if one is interested in understanding the systematic response of global temperatures to forcing.

3.2 A simple, physically-based model for the centennial-scale response to forcing

A common approach is to use more complex models, including full GCMs, to explain the systematic response of interest. (Model output is also used in concert with observations in the context of “detection and attribution” studies; see, e.g., Chapter 10 of IPCC (2013).) Some may object to this approach, however, out of a worry that the climate model has already been tuned to match the observed historical temperature trend or is otherwise conditioned on past temperature observations (Knutti, 2008; Huybers, 2010; Mauritsen et al., 2012). There is therefore value in a compromise approach between the linear time trend model and very complex numerical simulations. In this work, we discuss a statistical model that is easy to apply but that encodes some physical intuition for the problem that makes the model interpretable and hopefully applicable over longer time periods. The goal is to show that even simple models incorporating limited physical information can provide more insight about temperature trends and their uncertainties given the observed data than can regression models in time.

A very simplified physical model for the response to an instantaneous change in radiative forcing is that temperatures approach their new equilibrium in exponential decay. That is, writing $F_{\text{inst}}(t)$ for a step function that changes at time $t = 0$,

$$f(F_{\text{inst}}(t'); t' < t) \approx \mu_0 + \lambda(1 - \rho^t)\mathbf{1}\{t \geq 0\},$$

where λ is the change in equilibrium temperature, μ_0 is the mean temperature in the baseline state, and ρ controls the rate at which the changes in temperatures approach λ , taking values between zero (instantaneous response time) and one (infinite response time). Such a model can be interpreted as the solution to a simple energy balance model⁶. In reality, this is an overly simplified model because the Earth shows responses at multiple timescales (e.g., Held et al. (2010); Olivié et al. (2012); Geoffroy et al. (2013) and others). In any case, when convolved with a time-varying forcing trajectory, the resulting model for the systematic response is an infinite distributed lag model in the forcing trajectory with weights decaying exponentially (e.g., Caldeira and Myhrvold (2013); Castruccio et al. (2014)).

We propose the following model for the systematic temperature response in the observed data, a model similar to those used in Caldeira and Myhrvold (2013) and Castruccio et al. (2014):

$$f(F(t'); t' \leq t) \approx \mu_0 + \lambda_A h\left(\rho_A, \frac{F_A(t')}{F_{2\times}}; t' \leq t\right) + \lambda_N h\left(\rho_N, \frac{F_N(t')}{F_{2\times}}; t' \leq t\right), \quad (3)$$

where

$$h(\rho, x(t'); t' \leq t) = (1 - \rho) \sum_{k=0}^{\infty} \rho^k x(t - k).$$

In model (3), λ_A and λ_N represent “sensitivities” to anthropogenic and natural forcings, F_A and F_N , respectively, and have units of degrees Celsius temperature change per forcing change $F_{2\times}$ (the forcing associated with a doubling of atmospheric CO₂, approximately

⁶This simple model makes two assumptions: first, that the equilibrium temperature change is linear in the forcing (this is the so-called *linear forcing feedback model*; see Appendix A1), and second, that the rate of warming is approximately proportional to the heat uptake.

3.7 W/m²). The parameter λ_A is similar to the *equilibrium climate sensitivity*⁷, but will be estimated as somewhat lower than that quantity, in part because the proposed model contains only a single timescale of response to anthropogenic forcing (see Appendix A1). (Caldeira and Myhrvold (2013) and Castruccio et al. (2014) used multiple timescales in modeling longer series from GCM output, but we cannot distinguish these with only 136 years of data and given a smooth past trajectory of anthropogenic forcings.) Response timescales to anthropogenic and natural forcings are set by the parameters ρ_A and ρ_N (taking values between zero and one). Model (3) should approximate temperature trends reasonably well up to centennial timescales, but not at the millennial timescales at which the deep ocean mixes.

We separate natural and anthropogenic forcings in model (3) because they seem not strictly comparable (Figure 1, right). First, there is evidence that aerosol forcing from volcanic eruptions is less efficacious than CO₂ forcing (Sokolov, 2006; Hansen et al., 2005; Marvel et al., 2015); while we use estimates of effective radiative forcing, which should compensate for efficacy, these estimates do not include an adjustment for the volcanic forcing. Second, the timescales of response associated with these forcings may also be different, possibly because ocean heat content responds differently to sudden and/or negative changes in forcing (as produced by volcanic eruptions) compared to more gradual and/or positive changes (as in continued anthropogenic emissions of CO₂) (e.g., Gregory and Forster (2008); Padilla et al. (2011)). We combine solar and volcanic forcings out of convenience; the solar forcings do change more rapidly than the anthropogenic forcings, and in any case the magnitude of the changes in solar forcing is small.

To illustrate the use of model (3), we fit it to different segments of the observed global mean surface temperature record and we compare to the linear fits estimated over the same timeframes. Figure 2 shows the resulting fitted models using the data from 1970-2015, 1950-2015, and 1880-2015. The estimated trend from model (3) is relatively insensitive to the timeframe used. The estimated linear time trends, on the other hand, differ markedly using different timeframes, and agree with model (3) only after around 1970, during the time period over which net radiative forcing was evolving approximately linearly in time (see again Figure 1). The sensitivity of the inferred linear trend in global mean temperature to the starting date has been previously discussed (e.g., Liebmann et al. (2010)). These results suggest both that model (3) does indeed capture important aspects of the underlying physical processes driving temperature trends and that it therefore may be used to answer more interesting questions than can the linear time trend model.

4 Trend and uncertainty: what can we learn from applying our simple model to data?

In this section, we illustrate what can be learned by applying the simple model (3) to observed temperatures. To do this, we must introduce an additional model to capture natural variability ($\epsilon(t)$ in the assumed true model (1)). We then use our full model to infer the parameters in model (3), to evaluate their uncertainties given the data, and to explore the implications for understanding temperature trends.

To diagnose features of natural variability, spectral analysis is an intuitive framework,

⁷The change in equilibrium mean temperature associated with a doubling of CO₂ concentration.

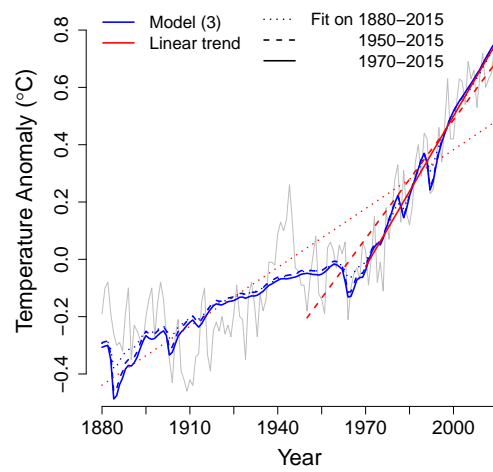


Figure 2: Comparison of the fitted values for model (3) and the linear time trend model fitted to the global mean temperature record over different timeframes. (The fitted model (3) trends are extended back to the 1880 regardless of the timeframe used to fit the model.) The linear model appears in agreement with model (3) roughly after 1970, but not before. By contrast, model (3) produces fairly stable estimates of the mean response during the 20th century, although we note that the apparent fit to the data may be slightly poorer in the earliest part of the record.

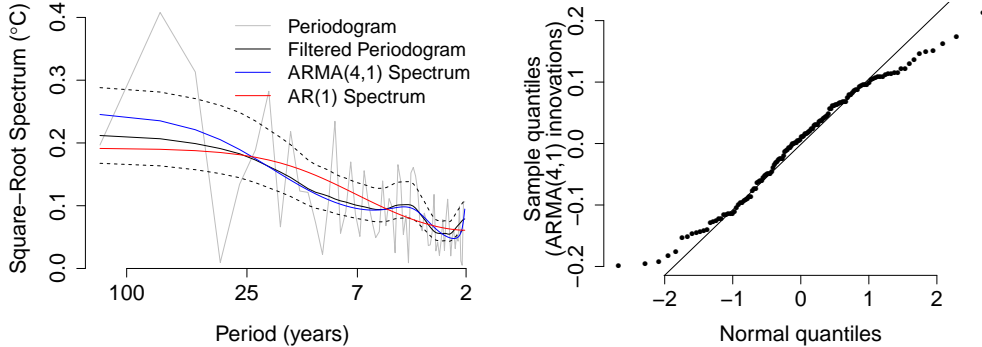


Figure 3: Left, the raw periodogram of the residuals from model (3), a filtered periodogram (twice applying a moving average of width 5), and the power spectra associated with fitted ARMA(4,1) and AR(1) models. The dashed lines are at ± 2 standard errors associated with the filtered periodogram. The ARMA(4,1) model appears to more realistically represent low-frequency variation in the residuals, which is crucial for inferences about trends. Right, normal quantile-quantile plot for the ARMA(4,1) sample innovations. There is some evidence that the innovations are light-tailed compared to the normal distribution.

since the frequency properties of natural variability are tied to uncertainties in trends: uncertainty in smooth trends is more strongly affected by low-frequency than high-frequency natural variability. Figure 3, left, shows the raw periodogram associated with the residuals from model (3) and a smoothed estimate of the spectrum. We also show the spectra associated with ARMA(4,1) and AR(1) model fits to the residuals, which are the models selected by AICc (Hurvich and Tsai, 1989) and BIC (Schwarz, 1978), respectively. Both the AICc and the BIC are common information criteria used for selecting time series models; the AICc is the AIC with a finite sample correction. (See Table A2 for the coefficient estimates, innovation standard deviations, and AICc and BIC associated with these two models.) Both models appear to fit the data reasonably well; the ARMA(4,1) model arguably overfits at the higher frequencies, but the AR(1) model may be underestimating variability at the lowest frequencies. Since low frequency variability is most important to uncertainties in smooth trends, we adopt the more conservative choice of using the ARMA(4,1) model. Figure 3, right, shows the normal quantile-quantile (Q-Q) plot for the sample innovations from this model; there is evidence that the innovations are somewhat more light-tailed than Gaussian, so standard errors based on a Gaussian assumption should not be overoptimistic.

Given the fully parametric model, combining (3) and a Gaussian ARMA(4,1) noise model, we proceed with uncertainty quantification through a parametric bootstrap (i.e., simulating under the fitted model). In a relatively short time series and given a smooth past trajectory of forcings, it is difficult to distinguish between a climate with both a high sensitivity (large value of λ) and slow response (large value of ρ) versus one with a lower sensitivity (smaller value of λ) but a faster response (smaller value of ρ). The estimates $\hat{\lambda}_A$ and $\hat{\rho}_A$ are therefore strongly dependent, with $\hat{\lambda}_A$ increasing explosively as $\hat{\rho}_A \rightarrow 1$ (Figure 4 shows their bivariate bootstrap distribution). The strong nonlinear relationship

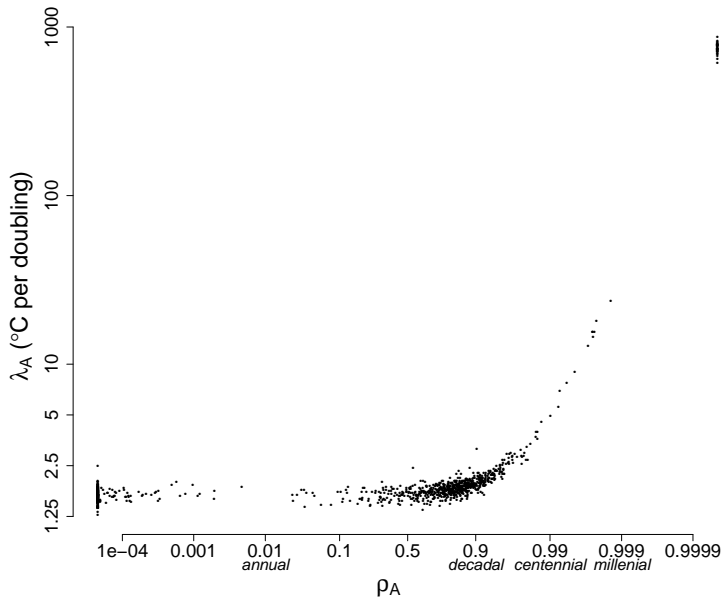


Figure 4: Distribution of the parametric bootstrap estimates of λ_A and ρ_A from model (3). It is difficult to distinguish between the rate of response and the sensitivity using only global mean temperatures from recent history.

between these two parameters, and the high degree of skewness in the marginal distribution of $\hat{\lambda}_A$, are the reasons that we rely on bootstrapping for uncertainty quantification, as the typical appeals to asymptotic normality are not viable in this setting.

In the following, we will represent uncertainties using the simple bootstrap percentile method. The percentile method is subject to criticism (e.g., Hall (1988)). We have found, however, that adjusting the percentile method using a nested bootstrap results in narrower confidence limits. For this reason, we believe that the raw percentile-based intervals may be conservative in this setting, so we choose to report the apparently conservative intervals. Our point estimates are based on a two-step procedure wherein model (3) is estimated via least squares and the ARMA(4,1) model is estimated via maximum likelihood on the residuals. While this procedure may be somewhat suboptimal compared to jointly estimating the mean and covariance structure, the two-step procedure is substantially faster, which is important for carrying out the nested bootstrap.

4.1 Uncertainties in the sensitivity parameters

When using the full 1880-2015 global mean surface temperature record, the point estimate for the sensitivity to anthropogenic forcing is $\hat{\lambda}_A = 1.8^\circ\text{C}$ per doubling, with $\hat{\rho}_A = 0.80$ (which implies mixing on decadal timescales). The estimated sensitivity to natural forcing is much smaller, $\hat{\lambda}_N = 0.21^\circ\text{C}$ per doubling with $\hat{\rho}_N = 0.58$. In this section, we discuss uncertainties in these estimates.

Using our statistical model, the historical data appear to provide a lower bound for λ_A (assuming for now that the forcings are known) but cannot rule out extremely large and

Percentile interval	$\hat{\lambda}_A = 1.8$		$\hat{\lambda}_N = 0.80$	
	Lower	Upper	Lower	Upper
5-95 (90%)	1.5	3.0	-0.15	1.5
2.5-97.5 (95%)	1.5	690	-1.1	4.1
0.5-99.5 (99%)	1.4	790	-13	490

Table 1: Parametric bootstrap percentile intervals for the sensitivities in model (3), λ_A and λ_N , to anthropogenic and natural sources, respectively (in units $^{\circ}\text{C}$ per doubling). The data appear to provide a lower bound for λ_A , but cannot rule out even implausibly large values; the very large values are associated with slow responses (see Figure 4). The data cannot rule out $\lambda_N = 0$, likely because there are few prominent volcanic eruptions in the historical record analyzed and the response to volcanic aerosols may be small.

implausible values on the order of tens or hundreds of degrees per doubling (the 2.5-97.5th bootstrap percentile interval is 1.5 to 690 $^{\circ}\text{C}$ per doubling). These very large values are not supported by evidence from the paleoclimate record (e.g., IPCC (2013) Chapter 5) and the approximation of the linear forcing feedback model, on which (3) implicitly relies, breaks down under high sensitivity (Bloch-Johnson et al., 2015). For the sensitivity to natural forcings, the data cannot rule out $\lambda_N = 0$ (the 2.5-97th bootstrap percentile interval is -1.1 to 4.1 $^{\circ}\text{C}$ per doubling). Table 1 gives some intervals at different percentiles for the parameters λ_A and λ_N . (The parameters ρ_A and ρ_N are essentially unconstrained by the data.)

The IPCC’s own 66% “likely” interval for equilibrium sensitivity is 1.5 $^{\circ}\text{C}$ to 4.5 $^{\circ}\text{C}$ per doubling, which subjectively combines estimates from various sources using multiple lines of evidence including from ensembles of models with different physics, and accounts for other sources of uncertainty that we have so far ignored, such as uncertainty in the forcings themselves (see IPCC (2013) 10.8.2 and Box 12.2). The bulk of the distribution of our estimate is somewhat narrower than the IPCC’s, likely because so far we have not accounted for uncertainty in radiative forcings; however, the IPCC rules out the very large and unphysical values in the right tail of our intervals. We here stress again that since we are estimating the centennial-scale response, the estimates of the sensitivity that we provide will tend to be lower than the equilibrium sensitivity estimated in the IPCC’s interval (see Appendix A1). Individual estimates of the equilibrium climate sensitivity and associated uncertainty in the literature are discussed in IPCC (2013) Section 10.8.2 (see also again Appendix A1).

The main source of uncertainty in the upper bound for λ_A is due to uncertainty in the “equilibration time” of the climate associated with smoothly increasing anthropogenic forcing, controlled by ρ_A . If we restrict ρ_A to, say, centennial scales or smaller, then the uncertainty is substantially decreased (see again Figure 4). While we may argue through other lines of evidence and reasoning that extremely large values of ρ_A and λ_A are implausible, the statistical model is being used to quantify the information content of the historical temperature record itself. This suggests that even our minimally informed model may be overly empirical for some purposes. The inability of the data to rule out $\lambda_N = 0$ is, on the other hand, probably due to the fact that there are few prominent volcanic eruptions in the historical record analyzed and that the response to volcanic aerosols may be small for the

reasons discussed above.

4.2 Uncertainties in near- and long-term trends

The uncertainties in the sensitivity and rate of response parameters imply greater uncertainties in projected longer-term future trends in global mean temperature than in the historical and near-term projected trends. To illustrate this, we examine the implied future trends under the hypothetical (extended) RCP8.5 scenario, in which radiative forcing increases and then stabilizes in the year 2150. We simulate new time series using our estimates of model (3) and the ARMA(4,1) noise model, given radiative forcings from this scenario. The projected trend and associated pointwise uncertainties are shown in Figure 5.

Projected mean temperatures, and especially their associated uncertainties, continue to increase even after stabilization of forcing. This is a consequence of the joint uncertainty in λ_A and ρ_A , and in particular of the inability to rule out implausible values of these parameters. If the goal, then, is to provide a long-term projection of mean temperatures given only the historical temperature record, these estimates will unsurprisingly be quite uncertain (even assuming known past and future forcings).

On the other hand, trends in the historical and near-term response are much more certain. The observations strongly suggest that mean temperatures increased in the 20th century: for example, the (2.5-97.5)-percentile interval for the mean response in the year 2000 (expressed compared to the 1951-1980 average) is well above zero at (0.4,0.6)°C. These kinds of distinctions between the uncertainty in the near- and longer-term mean responses are not easily made using a time trend model.

4.3 Decreasing uncertainty in the sensitivity parameter as more data is observed

We have shown that the short historical temperature record alone produces fairly uncertain estimates of the sensitivity parameter, λ_A in model (3) (Figure 4, Table 1), and therefore of longer-term temperature trends (Figure 5). We now examine how these uncertainties decrease as the temperature record increases (as in, e.g., Kelly and Kolstad (1999); Ring and Schlesinger (2012); Padilla et al. (2011); Urban et al. (2014); Myhre et al. (2015) and others). To do this, we artificially extend the temperature record by generating new synthetic time series using the mean and noise models estimated from the historical data and forcings from the same RCP8.5 scenario described above. We then reestimate model (3) for each synthetic series, using successively longer synthetic datasets. The results suggest that the data will not constrain the upper bound on the sensitivity parameter until another ~ 50 years, by which time (under our estimated model and the RCP8.5 scenario) temperatures will have already risen by about 3°C from the preindustrial climate. A summary of the evolution of uncertainties is given in Table 2.

These estimates could be more strongly constrained by using additional physical information. As discussed previously, the very high sensitivity estimates in the bootstrap distribution are cases where the estimated response time is unphysically long. Without external information about this timescale, however, long data records are required to rule out the large values of ρ_A and λ_A that the model entertains.

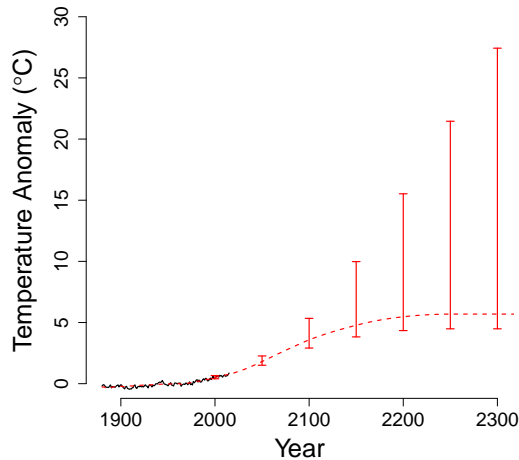


Figure 5: Projected mean temperature anomalies, and their uncertainties, under the RCP8.5 scenario, based on estimates from model (3) and assuming ARMA(4,1) noise. The black curve shows the observed temperatures. Intervals are pointwise (2.5-97.5)-percentile intervals. Radiative forcing stabilizes in the year 2250, but mean temperatures and especially their uncertainties continue to increase. While uncertainties in the long-term response are quite large, due largely to the inability to rule out implausible values of λ_A , the historical and near-term response is much more certain.

End year	(2.5-97.5)th percentile (°C per doubling)	Change in mean from preindustrial (°C)
2025	(1.5, 16)	1.3
2050	(1.6, 11)	2.2
2075	(1.6, 2.8)	3.1
2100	(1.7, 2.0)	3.9

Table 2: Evaluation of how uncertainty in the sensitivity parameter, λ_A , decreases as more data is observed, from simulations under the RCP8.5 scenario of future radiative forcing with an assumed value of $\lambda_A = 1.8^\circ\text{C}$ per doubling. The middle column shows the (2.5-97.5)th-percentile intervals for λ_A from simulations under the fitted model (3) and ARMA(4,1) noise. The rightmost column shows the increase in mean temperatures from the preindustrial climate under the fitted model at the year in question. Uncertainties in the upper bound of λ_A decrease relatively slowly as more data is observed.

4.4 Is there evidence of long memory natural variability in global mean temperatures?

One of the complicating factors in estimating trends in climate time series is the question of whether global mean temperatures exhibit *long memory*. Long memory processes have power spectra that behave like $(2 \sin(\omega/2))^{-2d}$ as the frequency $\omega \rightarrow 0$, with $d > 0$ (i.e., infinite power at the frequency zero); when $d < 1$ the process has finite total variance, as would be expected for a variable like global mean temperature. For more details on long memory processes, see Beran et al. (2013). By contrast, short-memory processes (like the ARMA(4,1) model we assume), have finite power at the origin. Many authors have suggested that natural temperature variability is well-modeled by processes with long memory but finite variance (e.g., Bloomfield (1992), Smith and Chen (1996), Gil-Alana (2005), Lennartz and Bunde (2009), Løvstetten and Rypdal (2016), and many others). Some authors have made a stronger claim that global mean temperatures are well-modeled by a random walk (e.g., Gordon (1991) and at least one standard time series textbook, Shumway and Stoffer (2013)), which would imply that global mean temperatures do not have a finite variance over time. In either case, if the Earth's temperatures exhibited long memory, it would be more difficult to estimate trends than in the short memory case, since low-frequency variability can be difficult to distinguish from trends.

The evidence for long memory, however, strongly depends on the assumed trend model. Many of the aforementioned authors draw their conclusions by assuming a linear time trend model and applying that model to the temperature record on durations of decades to over a century. As discussed previously, a linear trend model applied to a time series with a nonlinear trend will imply excessive low-frequency noise. Figure 6 shows the periodograms of the residual global mean temperatures after removing either a linear time trend or a trend of the form of (3). While the high-frequency behavior of the residuals is not much affected by the choice of trend model, the low-frequency behavior is very much affected. Apparent low-frequency variability is made more severe by assuming that mean temperatures increase linearly in time.

The question of long memory cannot be definitively settled using a dataset of only 136 observations, and other analyses make use of longer climate model runs or the paleoclimate record (e.g., Mann (2011)). Nevertheless, it should be clear that the linear time trend model is especially problematic for this purpose. In general, regression models in time, linear or otherwise, have a danger either of mistaking systematic trend for apparent low frequency variability (as just described), or of mistaking low-frequency variability for systematic trend (as would occur, for example, when using a nonparametric regression with too small of a smoothing bandwidth). Either can lead to misstated uncertainties, and therefore can be problematic even if the claim is that the trend model is only being used to test for significant warming and that the model is not believed to be true.

4.5 Implications of uncertain inputs: radiative forcing and temperatures

The analysis thus far has assumed that both radiative forcings and temperatures are known exactly, but uncertainty in the sensitivity and in trends also propagates from uncertainty in these quantities. We therefore discuss at least roughly the potential implications of imperfect knowledge of these inputs.

Of the two factors, uncertainty in radiative forcings, particularly from aerosols, is more

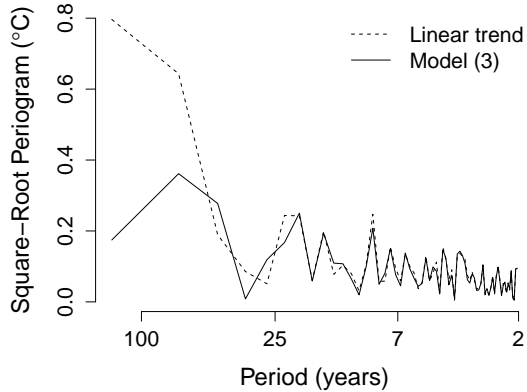


Figure 6: Raw periodograms of residuals from models (2) (dashed) and (3) (solid) fit to the full data record. There is substantially more low-frequency variability in the residuals from the linear trend model than in the residuals from model (3). Misspecified mean models will give a misleading impression of low-frequency variability, and therefore misleading uncertainties associated with the mean trend.

consequential, especially for the inferred lower bound of the sensitivity parameter from model (3). The importance of radiative forcing uncertainty for uncertainties in climate sensitivity has been widely noted (e.g., Gregory and Forster (2008); Padilla et al. (2011); Otto et al. (2013); Masters (2014); Lewis and Curry (2015); Myhre et al. (2015)). The trajectory of net effective radiative forcing from anthropogenic sources is poorly known; the IPCC states that the difference in net effective radiative forcing from anthropogenic sources between the years 2011 and 1750 was about 2.29 W/m^2 with a 95% confidence interval of 1.13 to 3.33 W/m^2 . We explore the implications of this uncertainty by simply scaling the entire trajectory of net radiative forcings from 1750 to the present such that the uncertainty in 2011 is as stated. Adjusting aerosol forcings to the high or low ends, respectively, produces sensitivity estimates from (3) varying by over a factor of two, from 1.2 to 3.7°C per doubling (vs. the original estimate 1.8°C). The aerosol uncertainty appears important: the value 1.2°C per doubling is lower than all of the bootstrap values of λ_A generated assuming known forcings (Figure 4 and Table 1).

Uncertainties in the global mean surface temperature record are comparatively less important. To partially address this issue, we re-estimate model (3) using each of the 100 ensemble members of the HadCRUT4 global mean temperature ensemble. The point estimates of λ_A range from 1.5 to 2.1°C per doubling, with estimates of ρ_A ranging from 0.79 to 0.90 . The point estimates of λ_N range from 0.71 to 20°C degrees per doubling, with estimates of ρ_N ranging from 0.86 to 0.996 . The additional uncertainty induced by observational uncertainty in the temperature record is smaller than either the uncertainty induced by natural variation in the temperature record or the uncertainty in radiative forcings.

5 Parametric vs. nonparametric uncertainty quantification

In Sections 3 and 4, we showed that characterizing the Earth’s systematic temperature response is better informed by making physical assumptions than by an ostensibly more empirical approach. In this section, we ask a similar question about characterizing natural variability, in settings similar to that discussed where data are temporally correlated and limited in length. We used a Gaussian ARMA(4,1) noise model in Section 4: is it more robust to assume a model for the noise, as we have done, or to adopt a nonparametric approach? The answer to this question depends on the length of the data record and the nature of the natural variability.

For the purposes of this illustration, we will use not the actual temperature record but rather some simple synthetic examples. We consider several artificial, trendless time series (the true mean of the process is constant) with temporally correlated noise, and evaluate the results of testing for a linear time trend (i.e., fitting model (2) and testing against the null hypothesis that $\beta = 0$) using different parametric (both correctly specified and not) and nonparametric methods for estimating uncertainties. The ordinary least squares standard errors, which assume uncorrelated noise, tend to be anticonservative (too small) and time series methods are supposed to ameliorate this overconfidence, but may or may not be successful in this regard depending on the context. The illustrations are simple but our conclusions should be relevant to actual data analysis and to more informed models.

We consider a few parametric approaches common in time series analysis. The typical practice is to assume that the noise follows a low order model, such as an ARMA model. Ideally, the noise model would be chosen in consultation with diagnostic plots and an information criterion like the AICc (as we do in Section 4). However, it is common practice to automatically select a model either solely by minimizing the AICc or another criterion, or just to assume a simple time series model, often the AR(1) model. Uncertainty in the trend parameter(s) can then be estimated in several ways. Usually, this is done assuming asymptotic normality for maximum likelihood estimators, and a test might be carried out using a t -statistic. If asymptotic normality is not viable, as for model (3), an alternative is to resort to using a parametric bootstrap (again as we do in Section 4) and to perform the test using bootstrap p -values.

We also evaluate the perhaps most typical nonparametric method for accounting for dependence in a time series, the block bootstrap (Kunsch, 1989). Here, residuals are resampled in blocks to generate bootstrap samples that retain much of the dependence structure in the original data. A popular variant is the circular block bootstrap (Politis and Romano, 1992), in which blocks can be overlapping and blocks starting at the end of the time series wrap back to the beginning. The block bootstrap has been a common method in the climate and atmospheric sciences for at least two decades (Wilks, 1997) and has been applied previously to test for time trends (or changes thereof) in the global mean surface temperature record. For example, Rajaratnam et al. (2015) argue that the circular block bootstrap gives better uncertainty estimates than does a parametric analysis in the setting of testing for a trend in a 16-year segment of the global mean temperature record.

While the block bootstrap works very well in some settings, the procedure is not free of assumptions. Like other variants of the nonparametric bootstrap, its justification is based on an asymptotic argument: for the block bootstrap to work well, the size of the block has to be small compared to the overall length of the data but large compared to the scale of the temporal correlation in the data. When the overall data record is short and natural

variability is substantially positively correlated in time, as for the historical temperature record, these dual goals may not both be achieved and we should not expect the block bootstrap to perform well.

In the following, we compare five methods (four parametric and one nonparametric) for generating nominal p -values testing for a significant linear time trend in trendless synthetic data: (a) a t -test assuming independent noise, (b) a t -test assuming Gaussian AR(1) noise with the model estimated via maximum likelihood, (c) bootstrap p -values from a parametric bootstrap assuming Gaussian AR(1) noise, (d) a t -test assuming Gaussian ARMA(p,q) noise with the order chosen by minimizing AICc, and (e) bootstrap p -values from a circular block bootstrap. We generate synthetic data from three different time series models, but in cases (b) and (c), the assumed parametric model is always AR(1). (Table A3 summarizes the models from which we simulate.) In cases (a), (b), and (d), the t -test degrees of freedom are approximated by $n - 2$ minus the number of parameters in the noise model. In case (e), we estimate p -values using a few different block lengths and show the results most favorable to the block bootstrap.

After generating nominal p -values, we evaluate the performance of the different methods. Since the null hypothesis is true in this artificial setting (the synthetic series are trendless), a correct p -value would be uniformly distributed. Deviations from the uniform distribution would then be a sign that the procedure generating the nominal p -value is uncalibrated. We therefore use Q-Q plots to compare the distribution of the simulated nominal p -values with the theoretical uniform distribution. Uncertainties are underestimated when the nominal p -value quantiles are smaller than the theoretical quantiles (i.e., when the Q-Q plot is below the one-to-one line). In this situation, inferences are anticonservative and the tests using the selected method will have Type I error rates that are larger than the nominal rate.

5.1 Parametric vs. nonparametric methods under a correctly specified noise model

We first compare the performance of the five methods for generating nominal p -values in the setting where the assumed AR(1) model is correctly specified (Figure 7). Unsurprisingly, pre-specified parametric time series methods give reasonably calibrated inferences when the parametric model is correctly specified (Figure 7, rows 2 and 3), although maximum likelihood gives somewhat anticonservative estimates of uncertainty with small sample sizes. The anticonservative bias of the maximum likelihood estimator can be reduced by instead using restricted maximum likelihood (REML) (e.g., McGilchrist (1989)) (see Appendix A5), but we focus here on the performance of maximum likelihood because it is more usually the procedure employed. It is also unsurprising that p -values under assumed independence are quite uncalibrated and anticonservative in this setting (Figure 7, top row), because standard errors are underestimated when positive temporal correlation is ignored.

It may, on the other hand, be surprising that automatically chosen parametric methods and nonparametric methods (blind selection via AICc and the block bootstrap, Figure 7, rows 4 and 5) can perform *even more poorly than assuming independence* if the sample size is very small. The AICc does improve on the AIC (not shown) by attempting to account for small sample biases, but still performs poorly in very small samples. The (nonparametric) block bootstrap is the worst-performing method at the smallest sample sizes while ostensibly based on the weakest assumptions. For either of these methods to perform comparably to the pre-specified parametric methods, sample sizes must be quite

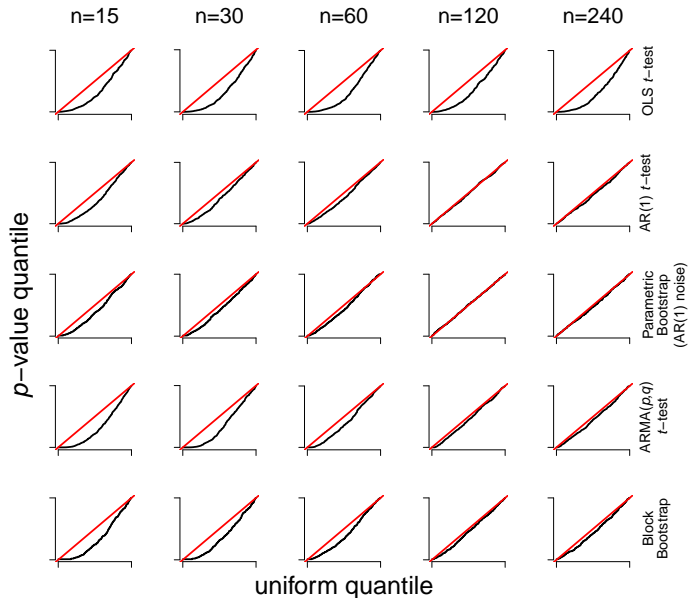


Figure 7: Quantile-quantile plots comparing the distribution of nominal p -values to the theoretical uniform distribution. Simulations are of mean zero, Gaussian AR(1) time series and p -values correspond to a two-sided test for a linear time trend. The length of the time series is given above each column. In the first row, the p -values are from the OLS t -test assuming independent noise; the second row is the t -test assuming AR(1) noise and the model fit via maximum likelihood; the third row uses a parametric bootstrap (again assuming AR(1) noise); the fourth row uses a t -test assuming ARMA(p,q) noise with the order of the model selected by AICc; and the last row uses a circular block bootstrap with block size chosen to be favorable to this method. The p -values calculated assuming the correct parametric model appear approximately correct for modest sample sizes and always outperform both blind selection by AICc and the block bootstrap. The latter two methods can be worse than assuming independence when sample sizes are very small.

large, indeed in this illustration larger than the available global mean temperature record. This should serve as a warning against using these methods for time series of modest length.

In actual practice, it can be advantageous, as we already discussed, to choose a noise model not automatically but in consultation with diagnostics (such as by comparing theoretical spectral densities with the empirical periodogram). In Section 4, we chose a noise model with consideration for the model’s representation of low-frequency variability. In that example, the chosen model did minimize the AICc, but gave more conservative inferences than the AR(1) model (which was chosen by BIC). The illustration above shows that this behavior is not generically true and that for small sample sizes it is dangerous to blindly select models by minimizing an information criterion alone.

5.2 Parametric vs. nonparametric methods under a misspecified model

The comparisons in the previous section were too favorable to the pre-specified parametric methods because the order of the specified noise model (an AR(1) model) was known to

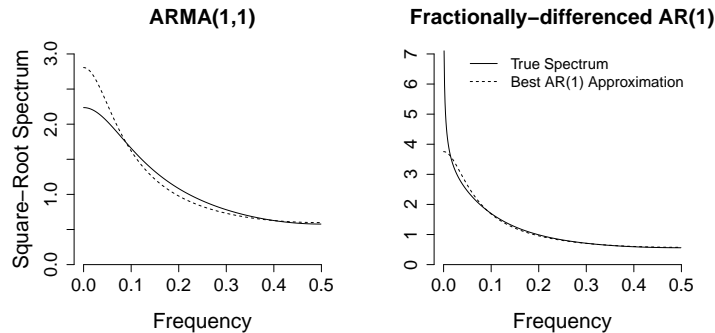


Figure 8: The power spectra associated with the two models from which we generate synthetic time series in Section 5.2, along with spectra of the best AR(1) approximations (in Kullback-Leibler divergence) to both models; see Table A3 for noise model parameters. The corresponding illustrations of the performance of the various time series methods are shown in Figures 9 and 10. The AR(1) model will tend to overestimate low-frequency variability in the first case and underestimate it in the second.

be correct. Now we compare these methods when the assumed noise model is misspecified. The performance of misspecified methods will depend in particular on how the misspecified model represents low- versus high-frequency variations in the noise process. Models that underestimate low-frequency variability will tend to be anticonservative for estimating uncertainties in smooth trends, whereas those that over-estimate low-frequency variability will tend to be conservative. We therefore repeat the illustrations in the previous section generating the synthetic time series from two different noise models (but still using the pre-specified AR(1) model to generate nominal p -values). The two models are chosen so that their best AR(1) approximations either under- or over-represent low-frequency variability. (Figure 8 shows the spectra corresponding to these two noise models and the best AR(1) approximation to each. See the Appendix, Table A3, for the model parameters and Section A3 for a comparison under an additional misspelled model.) The Q-Q plots corresponding to how the various time series methods perform in these two settings are shown in Figures 9 and 10.

First, we consider an ARMA(1,1) process whose best AR(1) approximation over-represents low-frequency variability (Figure 9). The results are similar to those when the model was correctly specified, except that at the largest sample sizes the pre-specified parametric methods slightly overestimate uncertainties, for the reasons discussed above. As before, both blind selection via AICc and the block bootstrap perform well for large sample sizes but very poorly for the smallest sample sizes.

Second, we consider a fractionally integrated AR(1) process; because this is a long-memory process, the best AR(1) approximation (and indeed any ARMA model) will severely under-represent low-frequency variability (Figure 10). All of the methods struggle in this setting and produce anticonservative estimates, but the pre-specified parametric methods still typically perform better than the ostensibly more flexible methods.

These results confirm that approaches to representing noise that appear to weaken assumptions are not guaranteed to outperform even misspecified parametric models. Mis-

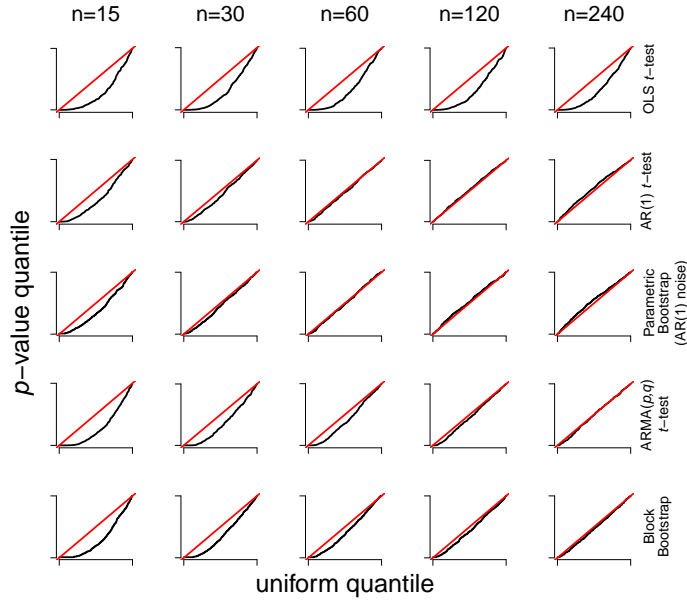


Figure 9: Same as Figure 7 but with simulations from an ARMA(1,1) model. The p -values calculated by incorrectly assuming an AR(1) model are increasingly conservative in larger sample sizes in this setting. Both blind selection via AICc and the block bootstrap are anticonservative for small sample sizes but improve as the sample size increases.

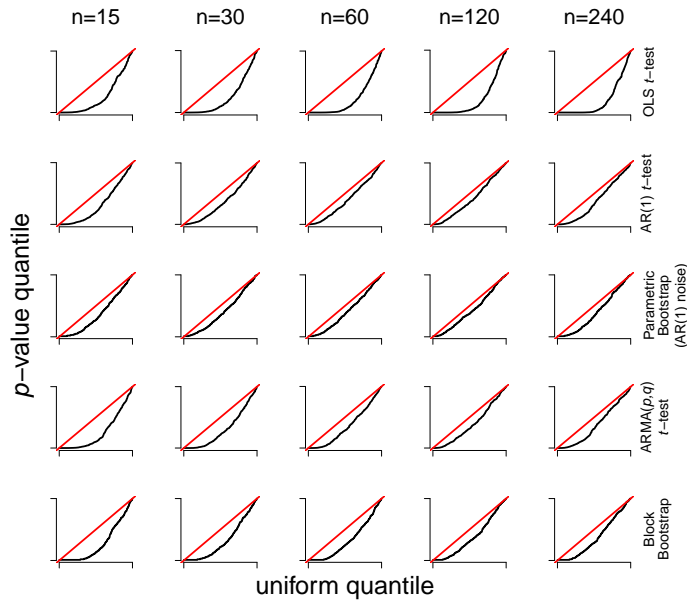


Figure 10: Same as Figure 7 but with simulations from a fractional AR(1) model. While none of the methods perform very well here, the incorrectly specified parametric methods are better, especially in smaller samples.

specified parametric models are most dangerous when low-frequency variability is under-represented, but methods like the block bootstrap will also have the most trouble when low-frequency variability is strong because very long blocks will be required to adequately capture the scale of dependence in the data. While it is crucial for the data analyst to scrutinize any assumed parametric model, we believe that in many settings when the time series is not very long, one will be better served by carefully choosing a low-order parametric model rather than resorting to nonparametric methods.

6 Discussion

We have shown that more targeted parametric modeling of trends and natural variability can provide for more informative and reliable analyses of the global mean temperature record than can more empirical methods. More empirical methods can fail to distinguish between systematic trends and natural variability, and can give seriously uncalibrated estimates of uncertainty; this is particularly the case in the setting of analyzing historical temperatures, where the data record is relatively short and temporal correlation is relatively strong.

The model we use in our analysis provides insights about the information contained in the historical temperature record relevant to both shorter-term and longer-term trend projections. The limited historical temperature record can provide information about shorter-term trends but unsurprisingly cannot constrain long-term projections very well; the past 136 years of temperatures simply do not alone contain the relevant information about equilibration timescales that would be required to constrain long-term projections. (Our analysis considers globally averaged temperatures; use of spatially disaggregated data may provide some additional information.) The distinction between uncertainties in shorter-term and longer-term projections, itself not easily made using a time trend model, serves to further illustrate that while the historical data record is an important source of information, it alone cannot be expected to answer the most important questions about climate change without bringing more scientific information to bear on the problem.

The purpose of this paper has been to illustrate these ideas in a particular, important scientific application. We believe that our discussion is illustrative of broader issues that arise in applied statistical practice, and will have particular relevance to problems involving trend estimation in the presence of temporally correlated data and in relatively data-limited settings. We suspect that many readers having engaged in the practice of applied statistics have felt personally the tension between targeted statistical modeling on the one hand and more empirical analyses on the other. One lucid discussion of the broader issues surrounding this tension can be found in the discussion of model formulation in Cox and Donnelly (2011). Empirical approaches have very successfully generated new insights and predictions in important areas, but there is a wide range of scientific problems where these approaches do not perform well and where targeted, domain-specific modeling is required. Statisticians can provide important insights into scientific problems; a crucial role for the statistician is to consider the modeling choices that will be both the most illuminating and the most reliable given the scientific questions and data at hand.

References

- Aldrin, M., M. Holden, P. Guttorp, R. B. Skeie, G. Myhre, and T. K. Berntsen (2012). Bayesian estimation of climate sensitivity based on a simple climate model fitted to observations of hemispheric temperatures and global ocean heat content. *Environmetrics* 23(3), 253–271.
- Armour, K. C., C. M. Bitz, and G. H. Roe (2013). Time-varying climate sensitivity from regional feedbacks. *Journal of Climate* 26(13), 4518–4534.
- Arrhenius, S. (1896). On the influence of carbonic acid in the air upon the temperature of the ground. *Philosophical Magazine Series 5* 41(251), 237–276.
- Beran, J., Y. Feng, S. Ghosh, and R. Kulik (2013). *Long-memory processes*. New York: Springer.
- Bloch-Johnson, J., R. T. Pierrehumbert, and D. S. Abbot (2015). Feedback temperature dependence determines the risk of high warming. *Geophysical Research Letters* 42(12), 4973–4980.
- Bloomfield, P. (1992). Trends in global temperature. *Climatic change* 21(1), 1–16.
- Cahill, N., S. Rahmstorf, and A. C. Parnell (2015). Change points of global temperature. *Environmental Research Letters* 10(8), 084002.
- Caldeira, K. and N. P. Myhrvold (2013). Projections of the pace of warming following an abrupt increase in atmospheric carbon dioxide concentration. *Environmental Research Letters* 8(3), 034039.
- Castruccio, S., D. J. McInerney, M. L. Stein, F. Liu Crouch, R. L. Jacob, and E. J. Moyer (2014). Statistical emulation of climate model projections based on precomputed gcm runs. *Journal of Climate* 27(5), 1829–1844.
- Cox, D. R. and C. A. Donnelly (2011). *Principles of applied statistics*. New York: Cambridge University Press.
- Easterling, D. R. and M. F. Wehner (2009). Is the climate warming or cooling? *Geophysical Research Letters* 36(8), L08706.
- Forest, C. E., P. H. Stone, and A. P. Sokolov (2006). Estimated pdfs of climate system properties including natural and anthropogenic forcings. *Geophysical Research Letters* 33(1), L01705.
- Foster, G. and S. Rahmstorf (2011). Global temperature evolution 1979-2010. *Environmental Research Letters* 6(4), 044022.
- Geoffroy, O., D. Saint-Martin, D. J. L. Olivié, A. Voldoire, G. Bellon, and S. Tytéca (2013). Transient climate response in a two-layer energy-balance model. part i: Analytical solution and parameter calibration using cmip5 aogcm experiments. *Journal of Climate* 26(6), 1841–1857.

- Gil-Alana, L. A. (2005). Statistical modeling of the temperatures in the northern hemisphere using fractional integration techniques. *Journal of Climate* 18(24), 5357–5369.
- Gluhovsky, A. (2011). Statistical inference from atmospheric time series: detecting trends and coherent structures. *Nonlinear Processes in Geophysics* 18(4), 537–544.
- Gordon, A. H. (1991). Global warming as a manifestation of a random walk. *Journal of Climate* 4(6), 589–597.
- Gregory, J. M. and P. M. Forster (2008). Transient climate response estimated from radiative forcing and observed temperature change. *Journal of Geophysical Research: Atmospheres* 113, D23105.
- Gregory, J. M., R. J. Stouffer, S. C. B. Raper, P. A. Stott, and N. A. Rayner (2002). An observationally based estimate of the climate sensitivity. *Journal of Climate* 15(22), 3117–3121.
- Hall, P. (1988). Theoretical comparison of bootstrap confidence intervals. *The Annals of Statistics* 16(3), 927–953.
- Hansen, J., R. Ruedy, M. Sato, and K. Lo (2010). Global surface temperature change. *Reviews of Geophysics* 48(4), RG4004.
- Hansen, J., M. Sato, R. Ruedy, L. Nazarenko, A. Lacis, G. Schmidt, G. Russell, I. Aleinov, M. Bauer, S. Bauer, et al. (2005). Efficacy of climate forcings. *Journal of Geophysical Research: Atmospheres* 110(D18).
- Held, I. M., M. Winton, K. Takahashi, T. Delworth, F. Zeng, and G. K. Vallis (2010). Probing the fast and slow components of global warming by returning abruptly to preindustrial forcing. *Journal of Climate* 23(9), 2418–2427.
- Hurvich, C. M. and C.-L. Tsai (1989). Regression and time series model selection in small samples. *Biometrika* 76(2), 297–307.
- Huybers, P. (2010). Compensation between model feedbacks and curtailment of climate sensitivity. *Journal of Climate* 23(11), 3009–3018.
- IPCC (2013). *Climate Change 2013: The Physical Science Basis. Contribution of Working Group I to the Fifth Assessment Report of the Intergovernmental Panel on Climate Change*. New York, NY: Cambridge University Press. Stocker, Thomas and Qin, Dahe and Plattner, Gian-Kasper and Tignor, M and Allen, Simon K and Boschung, Judith and Nauels, Alexander and Xia, Yu and Bex, Vincent and Midgley, Pauline M (eds.).
- Kelly, D. L. and C. D. Kolstad (1999). Bayesian learning, growth, and pollution. *Journal of economic dynamics and control* 23(4), 491–518.
- Knutti, R. (2008). Why are climate models reproducing the observed global surface warming so well? *Geophysical Research Letters* 35(18), L18704.
- Kunsch, H. R. (1989). The jackknife and the bootstrap for general stationary observations. *The Annals of Statistics* 17(3), 1217–1241.

- Lennartz, S. and A. Bunde (2009). Trend evaluation in records with long-term memory: Application to global warming. *Geophysical Research Letters* 36(16), L16706.
- Lewis, N. and J. A. Curry (2015). The implications for climate sensitivity of ar5 forcing and heat uptake estimates. *Climate Dynamics* 45(3), 1009–1023.
- Liebmann, B., R. M. Dole, C. Jones, I. Bladé, and D. Allured (2010). Influence of choice of time period on global surface temperature trend estimates. *Bulletin of the American Meteorological Society* 91(11), 1485–1491.
- Løvsletten, O. and M. Rypdal (2016). Statistics of regional surface temperatures post year 1900: long-range versus short-range dependence, and significance of warming trends. *Journal of Climate* 29(11), 4057–4068. in press.
- Mann, M. E. (2011). On long range dependence in global surface temperature series. *Climatic Change* 107(3), 267–276.
- Marvel, K., G. A. Schmidt, R. L. Miller, and L. S. Nazarenko (2015). Implications for climate sensitivity from the response to individual forcings. *Nature Climate Change* 6(4), 386–389.
- Masters, T. (2014). Observational estimate of climate sensitivity from changes in the rate of ocean heat uptake and comparison to cmip5 models. *Climate dynamics* 42(7), 2173–2181.
- Mauritsen, T., B. Stevens, E. Roeckner, T. Crueger, M. Esch, M. Giorgetta, H. Haak, J. Jungclaus, D. Klocke, D. Matei, et al. (2012). Tuning the climate of a global model. *Journal of Advances in Modeling Earth Systems* 4(3).
- McGilchrist, C. (1989). Bias of ml and reml estimators in regression models with arma errors. *Journal of Statistical Computation and Simulation* 32(3), 127–136.
- Meinshausen, M., S. J. Smith, K. Calvin, J. S. Daniel, M. Kainuma, J. Lamarque, K. Matsumoto, S. A. Montzka, S. C. B. Raper, K. Riahi, A. Thomson, G. J. M. Velders, and D. P. van Vuuren (2011). The rcp greenhouse gas concentrations and their extensions from 1765 to 2300. *Climatic Change* 109(1), 213–241.
- Morice, C. P., J. J. Kennedy, N. A. Rayner, and P. D. Jones (2012). Quantifying uncertainties in global and regional temperature change using an ensemble of observational estimates: The hadcrut4 data set. *Journal of Geophysical Research: Atmospheres* 117, D08101.
- Myhre, G., O. Boucher, F.-M. Bréon, P. Forster, and D. Shindell (2015). Declining uncertainty in transient climate response as co2 forcing dominates future climate change. *Nature Geoscience* 8(3), 181–185.
- Olivié, D. J. L., G. P. Peters, and D. Saint-Martin (2012). Atmosphere response time scales estimated from aogcm experiments. *Journal of Climate* 25(22), 7956–7972.
- Otto, A., F. E. L. Otto, O. Boucher, J. Church, G. Hegerl, P. M. Forster, N. P. Gillett, J. Gregory, G. C. Johnson, R. Knutti, et al. (2013). Energy budget constraints on climate response. *Nature Geoscience* 6(6), 415–416.

- Padilla, L. E., G. K. Vallis, and C. W. Rowley (2011). Probabilistic estimates of transient climate sensitivity subject to uncertainty in forcing and natural variability. *Journal of Climate* 24(21), 5521–5537.
- Politis, D. N. and J. P. Romano (1992). A circular block-resampling procedure for stationary data. In R. LePage and L. Billard (Eds.), *Exploring the limits of bootstrap*, pp. 263–270. New York: Wiley.
- Rajaratnam, B., J. Romano, M. Tsiang, and N. S. Diffenbaugh (2015). Debunking the climate hiatus. *Climatic Change* 133, 129–140.
- Riahi, K., S. Rao, V. Krey, C. Cho, V. Chirkov, G. Fischer, G. Kindermann, N. Nakicenovic, and P. Rafaj (2011). Rcp 8.5—a scenario of comparatively high greenhouse gas emissions. *Climatic Change* 109(1), 33–57.
- Ring, M. J. and M. E. Schlesinger (2012). Bayesian learning of climate sensitivity i: Synthetic observations. *Atmospheric and Climate Sciences* 2(4), 464–473.
- Rose, B. E. J., K. C. Armour, D. S. Battisti, N. Feldl, and D. D. B. Koll (2014). The dependence of transient climate sensitivity and radiative feedbacks on the spatial pattern of ocean heat uptake. *Geophysical Research Letters* 41(3), 1071–1078.
- Santer, B. D., C. Mears, C. Doutriaux, P. Caldwell, P. J. Gleckler, T. M. L. Wigley, S. Solomon, N. P. Gillett, D. Ivanova, T. R. Karl, et al. (2011). Separating signal and noise in atmospheric temperature changes: The importance of timescale. *Journal of Geophysical Research: Atmospheres* 116, D22105.
- Schwarz, G. (1978). Estimating the dimension of a model. *The Annals of Statistics* 6(2), 461–464.
- Shumway, R. H. and D. S. Stoffer (2013). *Time series analysis and its applications*. New York: Springer.
- Smith, R. L. and F.-L. Chen (1996). Regression in long-memory time series. In *Athens Conference on Applied Probability and Time Series Analysis*, pp. 378–391. New York: Springer.
- Sokolov, A. P. (2006). Does model sensitivity to changes in co2 provide a measure of sensitivity to other forcings? *Journal of climate* 19(13), 3294–3306.
- Urban, N. M., P. B. Holden, N. R. Edwards, R. L. Sriver, and K. Keller (2014). Historical and future learning about climate sensitivity. *Geophysical Research Letters* 41(7), 2543–2552.
- Wilks, D. S. (1997). Resampling hypothesis tests for autocorrelated fields. *Journal of Climate* 10(1), 65–82.
- Winton, M., K. Takahashi, and I. M. Held (2010). Importance of ocean heat uptake efficacy to transient climate change. *Journal of Climate* 23(9), 2333–2344.

A1 Implications for the transient climate response and equilibrium sensitivity

In this paper, we use the historical temperature record to estimate the trend model (3) that treats both the sensitivity parameter, λ_A , and the timescale of response parameter, ρ_A , as unknown. In this section, we compare our results to those from more commonly used methods of inferring the climate response from projections in climate models and of using the historical temperature record to estimate a climate sensitivity parameter.

Model (3) is justifiable over the relatively short (centennial) timescales over which the so-called *linear forcing-feedback model* is applicable. The linear forcing-feedback model says that the mean temperature response to an instantaneous forcing F behaves like $L\Delta T(t) \approx F - Q(t)$, where $\Delta T(t)$ is the change in mean temperature at time t from the baseline state, $Q(t)$ is the heat uptake (in W/m^2) at time t , and L is a climate response parameter (with units $\text{W}/\text{m}^2/\text{K}$). (In the context of this model, our sensitivity parameter is then $\lambda_A = F_{2\times}/L$.) Our method essentially infers $Q(t)$ by assuming that it decays exponentially until reaching zero again at equilibrium. The linear forcing-feedback model does not hold for all time, however, in part because both feedbacks and rates of warming vary spatially. In models, this typically results in additional warming over the millennial timescales on which the deep ocean mixes (e.g., Winton et al. (2010); Armour et al. (2013); Rose et al. (2014) and others). Additionally, climate feedbacks – and therefore climate sensitivity – may be state-dependent; this effect also typically amplifies global mean temperature rise (Bloch-Johnson et al., 2015). Collectively, this suggests that our sensitivity parameter λ_A will be smaller than the equilibrium climate sensitivity that measures the final, equilibrium temperature response.

We can compare the results of our model to reported results from GCMs by estimating the *transient climate response* (TCR), a popular metric of the short-term temperature response to forcing in climate models. The TCR is defined as the change in mean temperature after 70 years of a CO_2 concentration scenario that increases by 1% per year (so doubles after 70 years). In a multi-model comparison of these centennial-scale projections, IPCC (2013) reports a 66% “likely” interval for the TCR of 1.0 to 2.5°C. Our results from fitting model (3) to the historical data are fairly consistent with this: our estimate of the TCR is 1.7°C, with the 2.5-97.5th bootstrap percentile interval of 1.2 to 1.9°C. These intervals are not strictly comparable because the IPCC’s subjectively combines information from multiple lines of evidence. That said, our interval is shorter in part because it does not account for uncertainties in historical radiative forcings from anthropogenic aerosols. If we repeat the exercise of Section 4.5 (scaling the past radiative forcing trajectory), our central estimate of the TCR would be about 1.2°C if anthropogenic aerosols were on the high end and about 3.4°C if on the low end.

We can also compare our estimate of λ_A to prior estimates of a sensitivity parameter that also use the historical temperature record. The most typical approach in the literature shares some commonalities with our method, beginning with the same linear forcing-feedback model that implicitly underlies our analysis, but estimating a sensitivity parameter by using an additional observational estimate of global heat uptake. That is, studies use estimates of changes in forcing, F' , heat uptake Q' , and historical temperature change, $\Delta T'$, between a base a final period to compute $\hat{L} = (F' - Q')/\Delta T'$ and therefore $\hat{\lambda} = F_{2\times}\Delta T'/(F' - Q')$. Studies using this method include Gregory et al. (2002), Otto et al.

	Study	Best estimate (°C per doubling)	90% Interval (°C per doubling)
<i>Energy balance model using temperatures, forcing and heat uptake</i>	Gregory et al. (2002)	6.1	>1.6
	Otto et al. (2013)	2.0	1.2-3.9
	Masters (2014)	2.0	1.2-5.2
	Lewis and Curry (2015)	1.6	1.1-4.1
<i>Trend model (3)</i>	this work	1.8	1.5-3.0

Table A1: Comparison of estimates of a sensitivity parameter from studies that use observational data and a simple energy balance approach. The large best (median) estimate from Gregory et al. (2002) is due to a very fat right tail in their analysis; the mode of their distribution is 2.1°C per doubling. The estimates given in these studies are similar to our estimates of λ_A (which should be smaller than the equilibrium sensitivity).

(2013), Masters (2014), and Lewis and Curry (2015). The resulting sensitivity parameter estimate should be similar to our λ_A . Table A1 shows the results from these analyses. The uncertainty ranges given in these studies also tend to be slightly larger than the intervals we give for λ_A , again because these authors attempt to account for radiative forcing uncertainty in their analysis.

One advantage of this other, common approach is that it includes data about historical heat uptake, which is an additional, albeit uncertain, source of information that may improve estimates. However, since these methods do not involve an explicit trend model and require averaging the inputs over decadal or longer timespans, they cannot use the historical temperature record to estimate natural temperature variability. Most studies therefore estimate natural variability using climate model output, but climate models do not perfectly realistically represent even global annual mean temperature variability.

By contrast, an advantage of our approach is that it allows one to use the historical data to understand natural variability. Additionally, our approach allows one to answer questions about both historical trends and longer-term projections in the framework of one statistical model, whereas the approaches discussed above do not allow one to infer trends from increasing-in-time forcing scenarios. A disadvantage of our approach is that, as discussed above, we rely on the historical global mean temperature record to estimate the “equilibration” timescales (ρ_A and ρ_N), but the data contain little information about these quantities.

Regardless of the different advantages and disadvantages just discussed, both approaches to using the historical temperature record give similar results concerning the sensitivity parameter, and uncertainties in this parameter remain high. This demonstrates the limitations of the information content of the historical global mean temperature record alone for estimating longer-term projections of mean temperature changes. (As noted in Section 6, spatially disaggregated data may contain more information.)

A2 Coefficient estimates for noise model

Table A2 gives information about the ARMA(4,1) and AR(1) models fit to the residuals of model (3) used in Section 4. The ARMA(4,1) model give more conservative inferences

Model	Autoregressive parameters				Moving average parameter	Innovation standard deviation ($^{\circ}\text{C}$)	AICc	BIC
	ϕ_1	ϕ_2	ϕ_3	ϕ_4	θ_1			
ARMA(4,1)	-0.29 (0.19)	0.36 (0.12)	0.05 (0.09)	0.24 (0.09)	0.80 (0.19)	0.09	-258	-242
AR(1)	0.52 (0.07)	-	-	-	-	0.09	-257	-252

Table A2: Coefficient estimates (with standard errors in parentheses), innovation standard deviations, and AICc and BIC associated with ARMA(4,1) and AR(1) fits to the residuals from model (3). These two models minimize AICc and BIC, respectively. We use the ARMA(4,1) model because this model appears to better represent the low-frequency variation in the residuals (see Figure 3), which is crucial for inferences about trends.

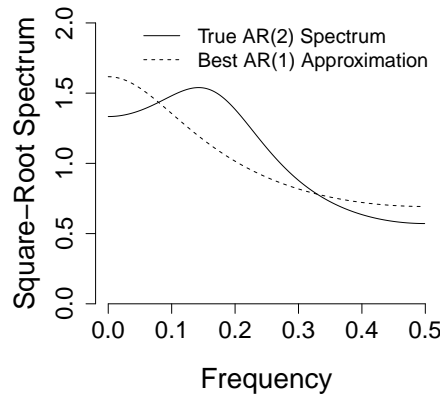


Figure A1: The power spectra associated with the AR(2) model from which we generate synthetic time series, along with spectrum of the best AR(1) approximation to each model (in Kullback-Leibler divergence); see Table A3 for noise model parameters.

about the systematic trend, and is the model we adopt in Section 4 (see Figure 3).

A3 Performance of misspecified methods under AR(2) simulations

In Section 5.2, we compared the five methods for generating nominal p -values in two settings where the pre-specified AR(1) model was incorrect, where the AR(1) model either over- or under-represented low-frequency variability. Here we present a third comparison, where the true noise model is an AR(2) model under which the AR(1) approximation over-represents variability at the lowest frequencies but under-represents variability at intermediate frequencies (Figure A1 shows the true spectrum and the best AR(1) approximation and Table A3, last row, gives the model parameters).

In this setting, all methods perform better than in the setting of Figure 9, but the relative

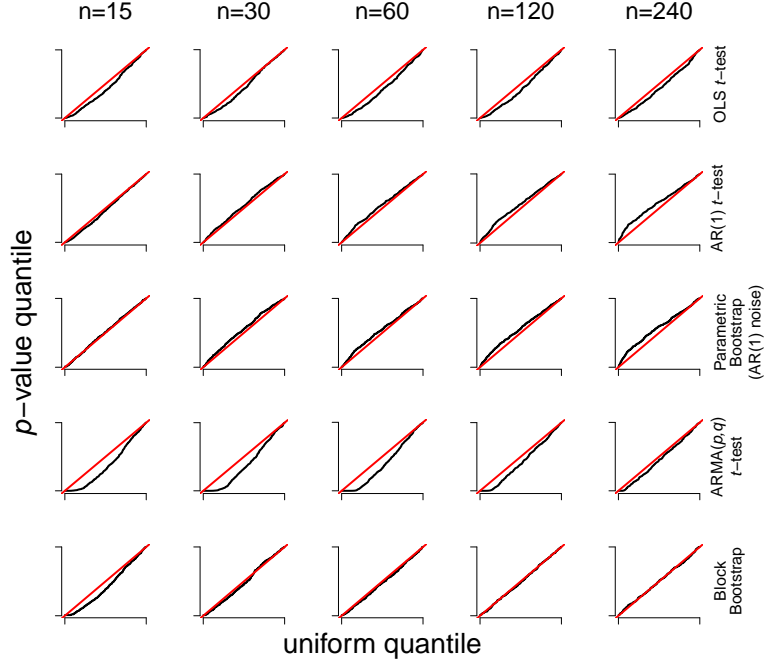


Figure A2: Same as Figure 7 but with simulations from an AR(2) model. The relative results are similar to the setting of Figure 9 but all methods perform better here.

performance of the different methods is largely the same as there, except that selection by AICc now performs even more poorly than the block bootstrap at the smallest sample sizes (Figure A2). This behavior again serves to emphasize that when making inferences about smooth trends, it is most crucial to represent low-frequency variability well.

A4 Model coefficients for simulations in Sections 5 and A3

In Sections 5 and A3, we generate synthetic, mean zero time series with different correlation structures. The models that we simulate from are summarized in Table A3. The general form for an autoregressive fractionally integrated moving average model (ARFIMA) of order (p, d, q) (of which all the simulated models are special cases) is

$$\left(1 - \sum_{k=1}^p \phi_k B^k\right) (1 - B)^d Y_t = \left(1 + \sum_{k=1}^q \theta_k B^k\right) \epsilon(t),$$

where Y_t is the time series at time t , the ϕ 's are the AR parameters, the θ 's are the MA parameters, d is the (fractional) differencing parameter, B is the backshift operator (i.e., $B^k Y_t = Y_{t-k}$), and $\epsilon(t)$ are uncorrelated innovations with constant variance. (The convention is that the acronym is shortened to account for parameters that are set to zero, so for example an ARFIMA(1,0,0) model is called an AR(1) model.)

Figure	Name	AR parameter(s)	MA parameter	Differencing parameter
7	AR(1)	0.5	0	0
9	ARMA(1,1)	0.5	0.25	0
10	fractional AR(1)	0.5	0	0.25
A2	AR(2)	(0.5,-0.25)	0	0

Table A3: Parameters in models from which we simulate in Sections 5 and A3.

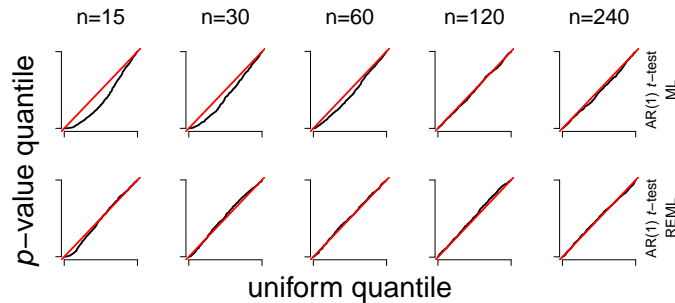


Figure A3: Comparison of maximum likelihood and REML in the same context as Figure 7. The first row is the same as the second row of Figure 7. In the second row here, the estimation is instead done using REML. The REML standard errors give better calibrated inferences in small sample sizes.

A5 Performance of maximum likelihood vs. REML

In Section 5, parametric inference was done using maximum likelihood estimators. As shown there, the MLE for covariance parameters can give anticonservative estimates of standard errors for trend parameters in small sample sizes. This problem can be substantially ameliorated using restricted maximum likelihood (REML) instead. Figure A3 repeats the tests in Section 5.1 (where both the true and assumed models are AR(1)) and compares the performance of maximum likelihood and REML. For larger sample sizes, the two procedures are comparable, but in small sample sizes REML is much better calibrated (although still slightly anticonservative in the smallest sample sizes).